

# Linear Constellation Precoding for OFDM With Maximum Multipath Diversity and Coding Gains

Zhiqiang Liu, *Member, IEEE*, Yan Xin, *Student Member, IEEE*, and Georgios B. Giannakis, *Fellow, IEEE*

**Abstract**—Orthogonal frequency-division multiplexing (OFDM) converts a frequency-selective fading channel into parallel flat-fading subchannels, thereby simplifying channel equalization and symbol decoding. However, OFDM's performance suffers from the loss of multipath diversity, and the inability to guarantee symbol detectability when channel nulls occur. In this paper, we introduce a linear constellation precoded OFDM for wireless transmissions over frequency-selective fading channels. Exploiting the correlation structure of subchannels and choosing system parameters properly, we first perform an optimal subcarrier grouping to divide the set of subchannels into subsets. Within each subset, a linear constellation-specific precoder is then designed to maximize both diversity and coding gains. While greatly reducing the decoding complexity and simplifying the precoder design, subcarrier grouping enables the maximum possible diversity and coding gains. In addition to reduced complexity, the proposed system guarantees symbol detectability regardless of channel nulls, and does not reduce transmission rate. Analytic evaluation and corroborating simulations reveal its performance merits.

**Index Terms**—Diversity methods, linear constellation precoding, orthogonal frequency-division multiplexing (OFDM).

## I. INTRODUCTION

RECENTLY, orthogonal frequency-division multiplexing (OFDM) has gained much attention as an effective multicarrier technique for wireless transmissions over frequency-selective fading channels. OFDM transforms a frequency-selective fading channel into parallel flat-fading subchannels, thereby significantly reducing the receiver complexity both in the equalization and the symbol decoding stages. However, the price paid for OFDM's simplicity is the loss of multipath diversity due to the fact that each symbol is transmitted over a single flat subchannel that may undergo fading, and the inability to guarantee symbol detectability when channel nulls occur on those subchannels. As a result, the performance of OFDM degrades if no additional countermeasures are taken. OFDM transmissions suffer also from high

peak-to-average ratio (PAR), which reduces the efficiency of high-power amplification.

Unlike OFDM, coded OFDM (C-OFDM) [21] is fading resilient, and has been adopted by many standards [2]. Typical choices for error-control codes include convolutional codes (see, e.g., [11]), and trellis-coded modulation (TCM) (see, e.g., [9]). TCM together with interleaving enables a better tradeoff between performance and bandwidth efficiency, while enjoying low-complexity Viterbi decoding. However, standard design paradigms for TCM make it difficult to design systems which achieve diversity gain equal to the code length.

This motivates the novel linear constellation precoded OFDM (LCP-OFDM) we develop in this paper for multicarrier transmissions over frequency-selective fading channels. Exploiting the correlation structure of the OFDM subchannels, we first perform what we term optimal subcarrier grouping that splits the set of correlated subchannels into subsets of less correlated subchannels. While greatly simplifying the decoder and the precoder design, subcarrier grouping turns out to be optimal in the sense of preserving maximum possible diversity and large coding gains. Within each subset of subcarriers, a linear constellation precoder (LCP) that is, in general, complex and could possibly be nonunitary is then designed to maximize both diversity and coding gains. The idea of using linear precoding to improve performance over fading channels is related to that of [1], [10] and [12], where a *real orthogonal* precoder is applied to maximize the channel cutoff rate [12], or maximize the minimum product distance [1], [10]. In addition to improved performance, LCP-OFDM does not reduce the transmission rate of uncoded OFDM, and guarantees symbol detectability (see also [16] and [17]). At the same time, its decoding complexity is approximately exponential in the channel order (or approximately polynomial if sphere decoding (SD) [15] is applied) that is often a relatively small number in practice. These merits of LCP-OFDM are confirmed by both analytical evaluation and extensive computer simulations. Interestingly, when each subset of subchannels has size equal to a power of two, our LCP-OFDM coincides with the coded modulation in [7]. Different from our goal of maximizing diversity and coding gains, the design objective in [7] is PAR reduction as well as performance enhancement through the design of nonstandard multidimensional signal sets.

The paper is organized as follows. In Section II, we describe the system model and state our problem. In Section III, we derive the performance of LCP-OFDM, in terms of maximum diversity and coding gains. To simplify the decoding, an optimal subcarrier grouping scheme is developed in Section IV. Section V deals with the design of LCPs, and Section VI compares LCP-OFDM with several competing alternatives. Several

Paper approved by C. Tellambura, the Editor for Modulation and Signal Design of the IEEE Communications Society. Manuscript received June 29, 2001. This work was supported in part by the National Science Foundation Wireless Initiative under Grant 9979442, in part by the Army Research Office under Grant DAAG55-98-1-0336, and in part by the Army Research Laboratory/Collaborative Technology Alliance (CTA) under Grant DAAD19-01-2-011. This paper was presented in part at the 35th Asilomar Conference on Signals, Systems, and Computers, Pacific Grove, CA, November 4–7, 2001.

Z. Liu is with the Department of Electrical and Computer Engineering, University of Iowa, Iowa City, IA 52244 USA (e-mail: zhiqiang-liu@uiowa.edu).

Y. Xin and G. B. Giannakis are with the Department of Electrical and Computer Engineering, University of Minnesota, Minneapolis, MN 55455 USA (e-mail: yxin@ece.umn.edu; georgios@ece.umn.edu).

Digital Object Identifier 10.1109/TCOMM.2003.809791

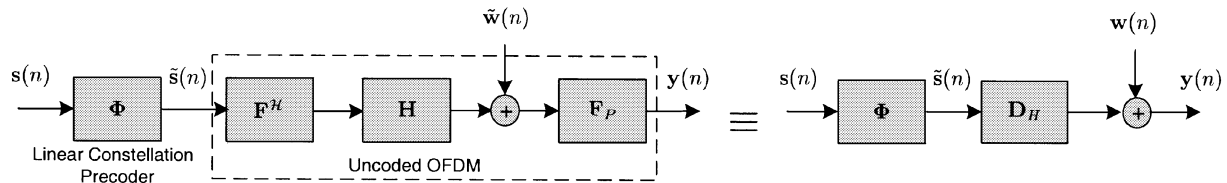


Fig. 1. LCP-OFDM and its equivalent block system.

practical issues are considered in Section VII. Simulations are carried out in Section VIII, while Section IX concludes this paper.

*Notation:* Column vectors (matrices) are denoted by boldface lower (upper) case letters. Superscripts  $T$  and  $\mathcal{H}$  stand for transpose and complex conjugate, respectively;  $\text{diag}(d_1, \dots, d_P)$  denotes a  $P \times P$  diagonal matrix with diagonal entries  $d_1, \dots, d_P$ ;  $\text{diag}(\mathbf{d})$  is a diagonal matrix with  $\mathbf{d}$  on its diagonal; and  $\mathbf{I}_P$  stands for the  $P \times P$  identity matrix.

## II. SYSTEM MODEL

We consider OFDM transmissions over frequency-selective fading channels. As depicted in Fig. 1, our LCP-OFDM consists of the serial concatenation of an LCP block followed by an (uncoded) OFDM modulator. The LCP is described by the  $P \times P$  matrix  $\Phi$  with entries over the complex field, that satisfies the transmit-power constraint  $\text{tr}(\Phi\Phi^{\mathcal{H}}) = P$ , with  $\text{tr}(\cdot)$  denoting matrix trace. The design of  $\Phi$  will be detailed in Section V. At the transmitter, information symbols  $s(n)$  belonging to the finite alphabet<sup>1</sup> (constellation set)  $\mathcal{A}_s$  are parsed into  $P \times 1$  blocks  $\mathbf{s}(n) := [s(nP), \dots, s(nP + P - 1)]^T$  that are sequentially processed by the LCP. Note that  $\Phi$  is square, and therefore, it does not reduce the transmission rate. After linear constellation precoding, the  $P \times 1$  precoded block  $\tilde{\mathbf{s}}(n) := [\tilde{s}(nP), \dots, \tilde{s}(nP + P - 1)]^T = \Phi\mathbf{s}(n)$  is treated as an OFDM symbol, and is transmitted using uncoded OFDM. Notice that  $\tilde{\mathbf{s}}(n)$  is generally a complex sequence no longer adhering to  $\mathcal{A}_s$  but to a larger size set  $\mathcal{A}_{\tilde{s}}$ . The LCP will be designed in Section V to maximize both diversity and coding gains.

A linear algebra approach to modeling uncoded OFDM has been introduced in [16], and we adopt it here as well; see also the dotted box in Fig. 1. The underlying frequency-selective channel is modeled as an  $L$ th-order finite-impulse response (FIR) filter, denoted as  $\mathbf{h} := [h(0), \dots, h(L)]^T$ , with  $h(l)$  standing for the  $l$ th channel tap. A cyclic prefix (CP) of length  $L_{\text{cp}} \geq L$  is inserted per transmitted OFDM block, and is removed from the corresponding received block to eliminate the interblock interference (IBI) induced by the FIR channel. As a result, the FIR channel vector  $\mathbf{h}$  is represented in our model (see Fig. 1) by the  $P \times P$  circulant matrix  $\mathbf{H}$  with  $(p, q)$ th entry  $[\mathbf{H}]_{p,q} = h((p - q) \bmod P)$ .

Let  $\mathbf{F}_P$  be the  $P \times P$  fast Fourier transform (FFT) matrix with  $[\mathbf{F}_P]_{p,q} = (1/\sqrt{P})\exp(-j2\pi(p - 1)(q - 1)/P)$ . Thanks to the circular structure of  $\mathbf{H}$ , performing inverse fast Fourier transform (IFFT) at the transmitter (post multiplication of  $\mathbf{H}$  by  $\mathbf{F}_P^{\mathcal{H}}$ ), and FFT at the receiver (premultiplication of  $\mathbf{H}$  by  $\mathbf{F}_P$ ), OFDM yields a diagonal equivalent channel matrix

$\mathbf{D}_H := \text{diag}(H(0), \dots, H(P - 1)) = \mathbf{F}_P\mathbf{H}\mathbf{F}_P^{\mathcal{H}}$  where  $H(p) := \sum_{l=0}^L h(l)\exp(-j2\pi lp/P)$  is nothing but the frequency response of the underlying FIR channel evaluated at the FFT grid (here  $j := \sqrt{-1}$ ).

Denote by  $\mathbf{y}(n) := [y(nP), \dots, y(nP + P - 1)]^T$  the  $P \times 1$  received block after FFT processing at the receiver, and  $\tilde{\mathbf{w}}(n) := [\tilde{w}(nP), \dots, \tilde{w}(nP + P - 1)]^T$  the  $P \times 1$  additive white Gaussian noise (AWGN) vector with correlation matrix  $\mathbf{R}_w = N_0\mathbf{I}_P$  where  $N_0$  is the noise power spectrum density normalized by the average symbol energy. With these notational for LCP-OFDM in matrix-vector form is (see Fig. 1)

$$\mathbf{y}(n) = \mathbf{D}_H\tilde{\mathbf{s}}(n) + \mathbf{w}(n) \quad (1)$$

or, equivalently

$$\mathbf{y}(n) = \mathbf{D}_H\Phi\mathbf{s}(n) + \mathbf{w}(n) \quad (2)$$

where the  $P \times 1$  FFT-processed noise vector  $\mathbf{w}(n) := [w(nP), \dots, w(nP + P - 1)]^T = \mathbf{F}_P\tilde{\mathbf{w}}(n)$  remains white with correlation matrix  $\mathbf{R}_w = N_0\mathbf{I}_P$  because the FFT matrix  $\mathbf{F}_P$  is unitary. Accounting for the CP, LCP-OFDM exhibits bandwidth efficiency  $\eta := P/(P + L_{\text{cp}})$ , which is equal to that of uncoded OFDM.

Given the received block  $\mathbf{y}(n)$ , we wish to decode  $\mathbf{s}(n)$  with maximum (multipath) diversity, large coding gains, and with low decoding complexity. These goals will be achieved by carefully designing the LCP matrix  $\Phi$ .

## III. PERFORMANCE BOUNDS OF LCP-OFDM

In this section we will address two basic questions: Q1) What is the maximum achievable diversity and coding gains for LCP-OFDM?; and Q2) What decoding complexity is required to achieve these gains?

We will first derive the maximum diversity and coding gains for LCP-OFDM. Exact bit-error rate (BER) performance analysis would be desirable, but it is difficult, if not impossible. Instead, we resort to the pairwise error probability (PEP) analysis that provides a good approximation for BER at high signal-to-noise ratio (SNR), and has been extensively used in communications; see, e.g., [5], [13], and [17]. Since PEP analysis is carried out within one block, we drop the block index  $n$  in (1) for notational simplicity. We assume that:

- A1) maximum-likelihood (ML) detection is performed with perfect channel state information (CSI) available at the receiver, but not at the transmitter; and
- A2) the channel vector  $\mathbf{h}$  is zero-mean, complex Gaussian with full rank correlation matrix  $\mathbf{R}_h := E(\mathbf{h}\mathbf{h}^{\mathcal{H}})$ .

Notice that A2) allows for correlated wireless channels with, e.g., an exponential power delay profile, as long as  $\mathbf{R}_h$  has full rank.

<sup>1</sup>In this paper,  $\mathcal{A}_s$  is normalized to have unit average energy.

Recalling (1) and dropping the block index  $n$ , we define the pairwise error event  $\{\tilde{\mathbf{s}} \rightarrow \tilde{\mathbf{s}}'\}$  with  $\tilde{\mathbf{s}} \neq \tilde{\mathbf{s}}'$  as the event that the receiver decodes  $\tilde{\mathbf{s}}'$  erroneously, when  $\tilde{\mathbf{s}}$  is actually transmitted, and denote by  $P(\tilde{\mathbf{s}} \rightarrow \tilde{\mathbf{s}}')$  the corresponding PEP. Similar to [5], [13], and [17], the conditional PEP is well approximated by

$$P(\tilde{\mathbf{s}} \rightarrow \tilde{\mathbf{s}}' | \mathbf{h}) \leq \exp \left[ -\frac{d^2(\mathbf{y}', \mathbf{y})}{4N_0} \right] \quad (3)$$

where  $\mathbf{y}' := \mathbf{D}_H \tilde{\mathbf{s}}'$ ,  $\mathbf{y} := \mathbf{D}_H \tilde{\mathbf{s}}$ , and  $d(\mathbf{y}', \mathbf{y}) = \|\mathbf{y}' - \mathbf{y}\|$  is the Euclidean distance between  $\mathbf{y}'$  and  $\mathbf{y}$ . Define the error vector  $\mathbf{e} := \tilde{\mathbf{s}}' - \tilde{\mathbf{s}} = \Phi(\mathbf{s}' - \mathbf{s})$ , where  $\tilde{\mathbf{s}}' := \Phi \mathbf{s}'$  and  $\tilde{\mathbf{s}} := \Phi \mathbf{s}$ . Exploiting the diagonal structure of  $\mathbf{D}_H$ , we obtain  $d^2(\mathbf{y}', \mathbf{y}) = \|\mathbf{D}_H \mathbf{e}\|^2 = \|\mathbf{D}_e \tilde{\mathbf{h}}\|^2$ , where  $\mathbf{D}_e := \text{diag}(\mathbf{e})$ , and  $\tilde{\mathbf{h}} := [H(0), \dots, H(P-1)]^T$  contains the channel response values on the FFT grid.

In order to link  $\tilde{\mathbf{h}}$  with  $\mathbf{h}$ , we define  $\mathbf{v}(p) := [1, \omega^p, \dots, \omega^{pL}]^T$  with  $\omega := \exp(-j2\pi/P)$ . By the definition of  $H(p)$ ,  $\mathbf{h}$  is related to  $\mathbf{h}$  via

$$\tilde{\mathbf{h}} = \mathbf{V}_P \mathbf{h} \quad (4)$$

where  $\mathbf{V}_P := [\mathbf{v}(0), \dots, \mathbf{v}(P-1)]^T$  is the  $P \times (L+1)$  truncated FFT (Vandermonde) matrix.

Because  $\mathbf{R}_h$  is positive definite Hermitian symmetric [c.f. A2)], we can decompose  $\mathbf{R}_h$  as  $\mathbf{R}_h = \mathbf{B}\mathbf{B}^H$ , where the  $(L+1) \times (L+1)$  matrix  $\mathbf{B} := \mathbf{R}_h^{1/2}$  is the square root of  $\mathbf{R}_h$  with full rank. Defining the prewhitened channel vector  $\tilde{\mathbf{h}} := [\tilde{h}(0), \dots, \tilde{h}(L)]^T = \mathbf{B}^{-1}\mathbf{h}$ , it then follows from A2) that  $\{\tilde{h}(l)\}_{l=0}^L$  are independent identically distributed (i.i.d.), zero-mean, complex Gaussian with unit variance. Taking into account (4), we can rewrite  $d^2(\mathbf{y}', \mathbf{y})$  as

$$d^2(\mathbf{y}', \mathbf{y}) = \|\mathbf{D}_e \tilde{\mathbf{h}}\|^2 = \mathbf{h}^H \mathbf{A}_e \mathbf{h} = \tilde{\mathbf{h}}^H \mathbf{C}_e \tilde{\mathbf{h}} \quad (5)$$

where the  $(L+1) \times (L+1)$  matrices  $\mathbf{A}_e := \mathbf{V}_P^H \mathbf{D}_e^H \mathbf{D}_e \mathbf{V}_P$  and  $\mathbf{C}_e := \mathbf{B}^H \mathbf{A}_e \mathbf{B}$ . As in [5], [13], and [17], we are interested in the average PEP over all possible random channel realizations. By averaging the PEP in (3) with respect to the random variables  $\tilde{h}(l)$ , we obtain the average PEP [5], [13], [17]

$$P(\tilde{\mathbf{s}} \rightarrow \tilde{\mathbf{s}}') \leq \prod_{l=0}^{R(\mathbf{C}_e)-1} \left( 1 + \frac{\lambda_l}{4N_0} \right)^{-1} \quad (6)$$

where  $\lambda_l, l = 0, \dots, R(\mathbf{C}_e) - 1$  are nonzero eigenvalues of  $\mathbf{C}_e$ , and  $R(\mathbf{C}_e)$  is the rank of  $\mathbf{C}_e$ . Assuming high SNR, it follows from (6) that

$$P(\tilde{\mathbf{s}} \rightarrow \tilde{\mathbf{s}}') \leq \left( G_{e,c} \frac{1}{4N_0} \right)^{-G_{e,d}} \quad (7)$$

where  $G_{e,d} := R(\mathbf{C}_e)$  and  $G_{e,c} := \left( \prod_{l=0}^{R(\mathbf{C}_e)-1} \lambda_l \right)^{1/R(\mathbf{C}_e)}$  are the pairwise diversity and coding gains, respectively, that depend on both  $\mathbf{e}$  and  $\Phi$ . It is clear from (7) that  $G_{e,d}$  and  $G_{e,c}$  affect the PEP bound in (7) in different ways:  $G_{e,d}$  determines how fast the average PEP decreases as the SNR increases, while  $G_{e,c}$  controls how this PEP shifts relative to the benchmark error-rate curve of  $(1/4N_0)^{-G_{e,d}}$ .

As mentioned earlier, both  $G_{e,d}$  and  $G_{e,c}$  depend on  $\mathbf{e}$ , or equivalently, on the choice of  $\mathbf{s}$  and  $\mathbf{s}'$ . Because  $s(n)$ 's are drawn from the finite constellation set  $\mathcal{A}_s$ , the set of all possible  $\mathbf{s}$ , denoted by  $\mathcal{A}_s^P$ , is also finite. Accounting for all possible pairwise errors, as in [17], we define herein the diversity and coding gains for LCP-OFDM, respectively, as

$$G_d := \min_{\mathbf{v} \neq \mathbf{0}} G_{e,d} \quad \text{and} \quad G_c := \min_{\mathbf{v} \neq \mathbf{0}} G_{e,c}. \quad (8)$$

Because the performance of LCP-OFDM depends on both  $G_d$  and  $G_c$ , it is important to maximize both  $G_d$  and  $G_c$ . Before specializing to particular  $\Phi$  designs, we next derive the maximum  $G_d$  and  $G_c$  achievable by LCP.

We have seen that  $G_d$  depends on  $\mathbf{C}_e$ . By checking the dimensionality of  $\mathbf{C}_e$ , it is clear that the maximum (and thus, optimum) diversity gain

$$G_{d,\max} = L + 1 \quad (9)$$

is achieved if and only if  $\forall \mathbf{s} \neq \mathbf{s}' \in \mathcal{A}_s^P$ , the matrix  $\mathbf{C}_e$  has full rank. Because the FIR channel  $\mathbf{h}$  has  $L+1$  taps, it is intuitively reasonable to expect that the diversity gain is no more than  $L+1$ . It is understood that with proper coding,  $G_{d,\max}$  can be also achieved by C-OFDM.

Suppose that  $\mathbf{C}_e$  has full rank, i.e.,  $R(\mathbf{C}_e) = L+1$ . By the definition of  $G_c$  in (8), we obtain

$$\begin{aligned} G_c &= \min_{\mathbf{v} \neq \mathbf{0}} [\det(\mathbf{C}_e)]^{\frac{1}{L+1}} \\ &= [\det(\mathbf{R}_h)]^{\frac{1}{L+1}} \cdot \min_{\mathbf{v} \neq \mathbf{0}} [\det(\mathbf{V}_P^H \mathbf{D}_e^H \mathbf{D}_e \mathbf{V}_P)]^{\frac{1}{L+1}} \end{aligned} \quad (10)$$

which implies that  $G_c$  is a function of the minimum determinant

$$\delta_{\text{lcp}} := \min_{\mathbf{v} \neq \mathbf{0}} \det(\mathbf{V}_P^H \mathbf{D}_e^H \mathbf{D}_e \mathbf{V}_P). \quad (11)$$

Let us define the LCP matrix  $\Phi := [\phi_1, \dots, \phi_P]^T := [\tilde{\phi}_1, \dots, \tilde{\phi}_P]$  where  $\phi_p^T$  ( $\tilde{\phi}_p$ ) is the  $p$ th row (column) of  $\Phi$ , and then write  $\mathbf{D}_e = \text{diag}[\phi_1^T(\mathbf{s}' - \mathbf{s}), \dots, \phi_P^T(\mathbf{s}' - \mathbf{s})]$ . By the definition of  $\mathbf{V}_P$  and  $\mathbf{D}_e$ , we find (12) as shown at the bottom of the page, where OT stands for other terms that are irrelevant at this point. Recalling that  $\text{tr}(\Phi^H \Phi) = \text{tr}(\Phi \Phi^H) = P$ , we

$$\mathbf{A}_e = \begin{bmatrix} \sum_{p=1}^P |\phi_p^T(\mathbf{s} - \mathbf{s}')|^2 & \text{OT} & \dots & \text{OT} \\ \text{OT} & \sum_{p=1}^P |\phi_p^T(\mathbf{s} - \mathbf{s}')|^2 & \dots & \text{OT} \\ \vdots & \vdots & \ddots & \vdots \\ \text{OT} & \text{OT} & \dots & \sum_{p=1}^P |\phi_p^T(\mathbf{s} - \mathbf{s}')|^2 \end{bmatrix} \quad (12)$$

have  $\sum_{p=1}^P \|\bar{\phi}_p\|^2 = P$ , and therefore,  $\min_{\forall p} \|\bar{\phi}_p\|^2 \leq 1$ . Because  $\mathbf{A}_e$  is positive definite, we can upper bound  $\delta_{\text{ICP}}$  by<sup>2</sup>

$$\begin{aligned} \delta_{\text{ICP}} &\leq \min_{\forall e \neq 0} \left[ \sum_{p=1}^P \left| \phi_p^T(\mathbf{s} - \mathbf{s}') \right|^2 \right]^{L+1} \\ &\leq \min_{\forall p} \|\bar{\phi}_p\|^{2(L+1)} \Delta_{\min}^{2(L+1)} \\ &\leq \Delta_{\min}^{2(L+1)} \end{aligned} \quad (13)$$

where  $\Delta_{\min}$  denotes the minimum Euclidean distance among constellation points in  $\mathcal{A}_s$ . It follows from (8), (10), and (13) that the maximum coding gain is

$$G_{c,\max} = [\det(\mathbf{R}_h)]^{1/(L+1)} \Delta_{\min}^2. \quad (14)$$

Note that the derivations of  $G_{d,\max}$  and  $G_{c,\max}$  do not restrict  $\Phi$  except for requiring  $\text{tr}(\Phi^H \Phi) = P$ . Thus, it is reasonable to treat  $G_{d,\max}$  and  $G_{c,\max}$  as performance bounds of LCP-OFDM.

In deriving performance bounds, we have assumed ML decoding. For a general precoder  $\Phi$ , LCP-OFDM transmits each information symbol over  $P$  subcarriers [c.f. (2)]. In other words, each received data symbol  $y(n)$  contains contributions from  $P$  information symbols. Thus, ML decoding has to involve an exhaustive search among  $|\mathcal{A}_s|^P$  possible  $\mathbf{s}(n)$ 's where  $|\mathcal{A}_s|$  is the cardinality of  $\mathcal{A}_s$ . In practical OFDM systems,  $P$  is typically large (e.g.,  $P = 64$  in HiperLan II [2]), and thus, ML decoding becomes computationally prohibitive. We next discuss how to reduce the decoding complexity by performing what we term subcarrier grouping.

#### IV. OPTIMAL SUBCARRIER GROUPING

In general, LCP-OFDM has high decoding complexity because every information symbol is transmitted over all  $P$  subcarriers. Our approach to reducing the decoding complexity is to divide the set of all subcarriers into nonintersecting subsets of subcarriers, and transmit every information symbol over subcarriers within only one of these subsets. We will term these subsets as subcarrier groups, and the resulting LCP-OFDM as grouped LCP-OFDM (GLCP-OFDM). Subcarrier grouping was originally suggested in [16] for multiuser interference elimination, and in [7] for PAR reduction. Here, the objective is different: we wish to reduce complexity while preserving performance. It will be shown that with considerably reduced complexity, the performance bounds in (9) and (14) still hold true for GLCP-OFDM if subcarrier grouping is properly designed. In addition to decoding simplicity, careful subcarrier grouping also brings about the simplicity of the LCP design, as we will detail in Section V.

##### A. Subcarrier Grouping

Let us rewrite (1) element-wise as

$$y(nP+p) = H(p)\check{s}(nP+p) + w(nP+p), \quad p \in [0, P-1] \quad (15)$$

which confirms that OFDM converts an FIR channel into a set of  $P$  flat subchannels with gains  $\{H(p)\}_{p=0}^{P-1}$ . Referring to  $H(p)$

<sup>2</sup>Here, we used the inequality  $\det(\mathbf{A}) \leq \prod_{i=1}^N a_{ii}$ , where  $a_{ii}$  is the  $i$ th diagonal entry of the  $N \times N$  positive definite matrix  $\mathbf{A}$ .

as the channel gain on the  $p$ th subcarrier, we introduce the set  $\mathcal{I} := \{0, 1, \dots, P-1\}$  to index the collection of  $P$  subcarriers. Choosing  $P = MK$ , subcarrier grouping can be represented by partitioning  $\mathcal{I}$  into  $M$  nonintersecting subsets  $\mathcal{I}_m := \{p_{m,1}, \dots, p_{m,K}\}$  each with cardinality  $K$ , i.e.

$$\begin{aligned} \mathcal{I}_1 \cup \mathcal{I}_2 \cup \dots \cup \mathcal{I}_M &= \mathcal{I} \\ \mathcal{I}_m \cap \mathcal{I}_{m'} &= \emptyset, \quad \forall m \neq m' \end{aligned} \quad (16)$$

where  $\emptyset$  denotes the empty set.

To link  $\mathcal{I}_m$  with the operation of subcarrier grouping, we further define for the  $m$ th group the subcarrier selector matrix  $\Psi_m := \mathbf{I}_P(\mathcal{I}_m, \cdot)$ , where  $\mathbf{I}_P(\mathcal{I}_m, \cdot)$  is a  $K \times P$  permutation matrix built from the  $\{p_{m,k} + 1\}_{k=1}^K$  rows of  $\mathbf{I}_P$ . Because each subcarrier is uniquely associated with one  $\check{s}(n)$ ,  $K$  subcarriers in  $\mathcal{I}_m$  are thus associated with  $K$  symbols  $\{\check{s}(nP + p_{m,k})\}_{k=1}^K$  that can be collected into a  $K \times 1$  block  $\check{\mathbf{s}}_m(n) := [\check{s}(nP + p_{m,1}), \dots, \check{s}(nP + p_{m,K})]^T = \Psi_m \check{\mathbf{s}}(n)$ . Letting  $\mathbf{y}_m(n) := \Psi_m \mathbf{y}(n)$ , it follows from (1) that

$$\mathbf{y}_m(n) = \mathbf{D}_{m,H} \check{\mathbf{s}}_m(n) + \mathbf{w}_m(n), \quad m \in [1, M] \quad (17)$$

where  $\mathbf{D}_{m,H} := \text{diag}[H(p_{m,1}), \dots, H(p_{m,K})] = \Psi_m \mathbf{D}_H \Psi_m^T$  and  $\mathbf{w}_m(n) := \Psi_m \mathbf{w}(n)$ . As mentioned earlier, we will reduce decoding complexity by transmitting each information symbol over only one of the  $M$  subcarrier groups. Mathematically, we divide  $\mathbf{s}(n)$  into  $M$  blocks  $\mathbf{s}_m(n) = \Psi_m \mathbf{s}(n)$ ,  $m \in [1, M]$ , and link  $\check{\mathbf{s}}_m(n)$  with  $\mathbf{s}_m(n)$  as follows:

$$\check{\mathbf{s}}_m(n) = \Theta \mathbf{s}_m(n), \quad m \in [1, M] \quad (18)$$

where the  $K \times K$  complex matrix  $\Theta$  constitutes the so-termed GLCP that will be designed in Section V. Clearly,  $\check{s}(nP + p_{m,k})$  is transmitted over subcarriers in  $\mathcal{I}_m$  only. In order to control the transmit power, we again impose the constraint  $\text{tr}(\Theta^H \Theta) = K$ . Combining (18) with (17), GLCP-OFDM is modeled as

$$\mathbf{y}_m(n) = \mathbf{D}_{m,H} \Theta \mathbf{s}_m(n) + \mathbf{w}_m(n), \quad m \in [1, M]. \quad (19)$$

To link GLCP-OFDM to LCP-OFDM modeled in (2), we stack the equations in (18) to obtain

$$\begin{bmatrix} \Psi_1 \\ \vdots \\ \Psi_M \end{bmatrix} \check{\mathbf{s}}(n) = \begin{bmatrix} \Theta \Psi_1 \\ \vdots \\ \Theta \Psi_M \end{bmatrix} \mathbf{s}(n).$$

Notice that  $\Phi$  in (2) can be expressed as

$$\Phi = \sum_{m=1}^M \Psi_m^T \Theta \Psi_m. \quad (20)$$

Clearly, designing GLCP-OFDM is equivalent to designing LCP-OFDM with the particular precoder  $\Phi$  specified in (20).

##### B. Designing Optimal Subcarrier Groups

By analyzing the diversity and coding gains of GLCP-OFDM, we design here optimal subcarrier grouping with the goal of reducing decoding complexity as much as possible, while preserving the maximum diversity and coding gains that we derived in Section III.

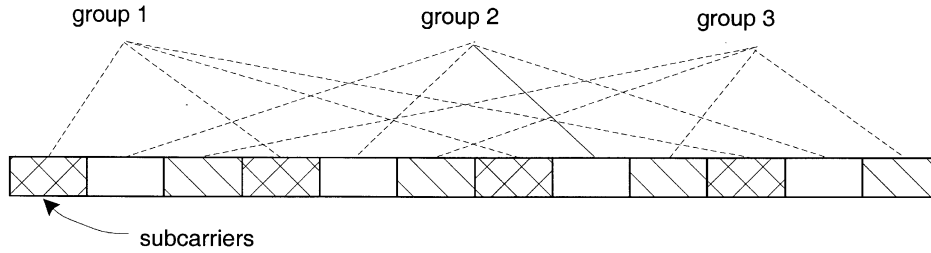


Fig. 2. Optimal subcarrier grouping ( $M = 3, L + 1 = 4$ ).

Let us drop the block index  $n$  in (17) and (19), and define

$$\begin{aligned} \mathbf{U}_m &:= [\mathbf{v}(p_{m,1}), \dots, \mathbf{v}(p_{m,K})]^T \quad K \times (L+1) \\ \mathbf{e}_m &:= \Theta(\mathbf{s}_m - \mathbf{s}'_m) \quad K \times 1 \\ \mathbf{D}_{m,e} &:= \text{diag}(\mathbf{e}_m) \quad K \times K \\ \mathbf{A}_{m,e} &:= \mathbf{U}_m^H \mathbf{D}_{m,e}^H \mathbf{D}_{m,e} \mathbf{U}_m \quad (L+1) \times (L+1). \end{aligned} \quad (21)$$

Mimicking the steps used to derive (7), the diversity gain of GLCP-OFDM can be expressed as

$$G_{m,d} := \min_{\forall \mathbf{e}_m \neq \mathbf{0}} R(\mathbf{A}_{m,e}). \quad (22)$$

By checking the dimensionality of  $\mathbf{A}_{m,e}$ , it is clear that the maximum diversity gain is  $G_{d,\max} = L+1$ , which is achieved if and only if  $\mathbf{A}_{m,e}$  has full rank, i.e.,  $R(\mathbf{A}_{m,e}) = L+1$ . In order to ensure  $R(\mathbf{A}_{m,e}) = L+1$ , one necessary condition is  $K \geq L+1$ . As assumed in A1), we will recover  $\mathbf{s}_m(n)$  from  $\mathbf{y}_m(n)$  by ML decoding, whose complexity is exponential in  $K$ . To minimize decoding complexity while preserving maximum diversity gain, it is practically preferable to choose  $K = L+1$ . Observe that  $\mathbf{U}_m$  is a Vandermonde matrix, and thus,  $\mathbf{A}_{m,e}$  will have full rank if and only if  $\mathbf{D}_{m,e}$  has full rank. Ensuring that  $\mathbf{D}_{m,e}$  has full rank for all possible distinct  $\mathbf{s}_m$  and  $\mathbf{s}'_m$  depends on the design of  $\Theta$  that will be addressed in Section V.

Suppose that  $\mathbf{A}_{m,e}$  has full rank and  $K = L+1$  is chosen. Proceeding along the lines used to arrive at (10), we find that the coding gain of GLCP-OFDM is given by

$$\begin{aligned} G_{m,c} &= [\det(\mathbf{R}_h)]^{\frac{1}{K}} [\det(\mathbf{U}_m^H \mathbf{U}_m)]^{\frac{1}{K}} \left[ \min_{\forall \mathbf{e}_m \neq \mathbf{0}} [\det(\mathbf{D}_{m,e}^H \mathbf{D}_{m,e})] \right]^{\frac{1}{K}} \end{aligned} \quad (23)$$

whose value depends on

$$\xi_{sc} := \det(\mathbf{U}_m^H \mathbf{U}_m)$$

and

$$\xi_{lcp} := \min_{\forall \mathbf{e}_m \neq \mathbf{0}} \det(\mathbf{D}_{m,e}^H \mathbf{D}_{m,e}).$$

In order to maximize  $G_{m,c}$ , both  $\xi_{sc}$  and  $\xi_{lcp}$  need to be maximized. How to maximize  $\xi_{lcp}$  depends on the design of  $\Theta$  that will be addressed in Section V. Note also that channel correlation will not affect this design, as long as  $\mathbf{R}_h$  has full rank. Here, we will address the maximization of  $\xi_{sc}$  by judiciously designing  $\mathcal{I}_m$ .

Let us consider a particular subcarrier grouping

$$\mathcal{I}_{m,\text{opt}} = \{m-1, M+m-1, \dots, (K-1)M+m-1\}. \quad (24)$$

For this grouping, we find that  $\mathbf{U}_m = \mathbf{V}_K \text{diag}(1, \dots, \omega^{L(m-1)})$ , and thus,  $\xi_{sc} = K^K$ . On the other hand, for arbitrary subcarrier grouping, it follows that  $\text{tr}(\mathbf{U}_m^H \mathbf{U}_m) = (L+1)^2$ . Since  $\mathbf{U}_m$  has full rank,  $\mathbf{U}_m^H \mathbf{U}_m$  is positive definite. Thus, the maximum  $\xi_{sc}$  for arbitrary subcarrier grouping will be  $\leq K^K$ . From this, we deduce that the subcarrier grouping specified in (24) is optimal in terms of maximizing  $G_{m,c}$ , and will, thus, be adopted henceforth. The optimal subcarrier grouping is illustrated in Fig. 2.

On the other hand, mimicking the derivation of (13), it can be readily proved that

$$\xi_{lcp} \leq \left[ \frac{\Delta_{\min}^2}{K} \right]^K. \quad (25)$$

Therefore, the maximum coding gain of GLCP-OFDM is  $[\det(\mathbf{R}_h)]^{1/(L+1)} \Delta_{\min}^2$ , which is identical to the maximum coding gain offered by LCP-OFDM.

Thus far, we have shown that GLCP-OFDM with optimal subcarrier grouping offers the potential to achieve the same maximum multipath diversity and coding gains as those of LCP-OFDM, while reducing the decoding complexity considerably if a small  $K$  is chosen. However, it is important to point out at the outset that subcarrier grouping preserves only maximum diversity and coding gains, and does not necessarily preserve the BER performance. The reason is twofold: 1) the PEP is only a good approximation of the BER performance at high SNR; and 2) in addition to diversity and coding gains, other factors such as the kissing number also affect the BER performance [1]. Having designed our optimal subcarrier grouping, we proceed to design  $\Theta$  in (18) to optimize our system.

## V. GLCP DESIGN

Subcarrier grouping reduces the design of LCP-OFDM to that of GLCP-OFDM. Consequently, the performance of LCP-OFDM is now up to the optimal design of the GLCP matrix  $\Theta$ . As mentioned in Section IV, the design criteria for  $\Theta$  can be summarized as follows.

- C1) *Maximum Diversity Gain Criterion.* Design a  $K \times K$  matrix  $\Theta$  with  $\text{tr}(\Theta \Theta^H) = K$  such that  $\forall k \in [1, K]$

$$\left| \boldsymbol{\theta}_k^T (\mathbf{s} - \mathbf{s}') \right| \neq 0, \quad \forall \mathbf{s} \neq \mathbf{s}' \in \mathcal{A}_s^K$$

where  $\boldsymbol{\theta}_k^T$  denotes the  $k$ th row of  $\Theta$ ; and  $\mathbf{s}$  and  $\mathbf{s}'$  are two  $K \times 1$  vectors with elements drawn from  $\mathcal{A}_s$ .

TABLE I  
 DESIGN EXAMPLES OF  $\Theta$  FOR  $K = 2, 3, \dots, 8$ 

$K$	$\alpha_1$	$\alpha_2$	$\alpha_3$	$\alpha_4$	$\alpha_5$	$\alpha_6$	$\alpha_7$	$\alpha_8$
2	$e^{-j\frac{\pi}{4}}$	$e^{-j\frac{5\pi}{4}}$						
3	$\sqrt[3]{2} e^{-j\frac{\pi}{12}}$	$\sqrt[3]{2} e^{-j\frac{9\pi}{12}}$	$\sqrt[3]{2} e^{-j\frac{17\pi}{12}}$					
4	$e^{-j\frac{\pi}{8}}$	$e^{-j\frac{5\pi}{8}}$	$e^{-j\frac{9\pi}{8}}$	$e^{-j\frac{13\pi}{8}}$				
5	$\sqrt[5]{2} e^{-j\frac{\pi}{20}}$	$\sqrt[5]{2} e^{-j\frac{9\pi}{20}}$	$\sqrt[5]{2} e^{-j\frac{17\pi}{20}}$	$\sqrt[5]{2} e^{-j\frac{25\pi}{20}}$	$\sqrt[5]{2} e^{-j\frac{33\pi}{20}}$			
6	$e^{-j\frac{2\pi}{7}}$	$e^{-j\frac{4\pi}{7}}$	$e^{-j\frac{6\pi}{7}}$	$e^{-j\frac{8\pi}{7}}$	$e^{-j\frac{10\pi}{7}}$	$e^{-j\frac{12\pi}{7}}$		
7	$\sqrt[7]{2} e^{-j\frac{\pi}{28}}$	$\sqrt[7]{2} e^{-j\frac{9\pi}{28}}$	$\sqrt[7]{2} e^{-j\frac{17\pi}{28}}$	$\sqrt[7]{2} e^{-j\frac{25\pi}{28}}$	$\sqrt[7]{2} e^{-j\frac{33\pi}{28}}$	$\sqrt[7]{2} e^{-j\frac{41\pi}{28}}$	$\sqrt[7]{2} e^{-j\frac{49\pi}{28}}$	
8	$e^{-j\frac{\pi}{16}}$	$e^{-j\frac{5\pi}{16}}$	$e^{-j\frac{9\pi}{16}}$	$e^{-j\frac{13\pi}{16}}$	$e^{-j\frac{17\pi}{16}}$	$e^{-j\frac{21\pi}{16}}$	$e^{-j\frac{25\pi}{16}}$	$e^{-j\frac{29\pi}{16}}$

C2) *Maximum Coding Gain Criterion.* Design a  $K \times K$  matrix  $\Theta$  with  $\text{tr}(\Theta\Theta^H) = K$  to maximize

$$\xi_{\text{lcp}} = \min_{\forall s \neq s'} \prod_{k=1}^K \left| \theta_k^T (s - s') \right|^2.$$

Note that when C2) is satisfied, C1) will be automatically satisfied.

Based on a design criterion similar to C2), a number of approaches have been proposed to design LCPs in the literature [1], [4], [6], [19], [20]. Among them, we are particularly interested in the *unified* algebraic construction method LCP-A [20, Sect. III-B] that was proposed in the context of multiple-antenna systems. Our design of optimal  $\Theta$  will follow the steps in [20] with appropriate modifications. For brevity, we just state the basic results pertaining to our context (readers are referred to [20] for detailed derivations and other algebraic construction methods).

#### A. Algebraic GLCP Construction

LCP-A constructs the GLCP matrix  $\Theta$  that applies to any  $K$ , and quadrature amplitude modulation (QAM), pulse-amplitude modulation (PAM), binary phase-shift keying (BPSK), and quaternary phase-shift keying (QPSK) constellations. Earlier constructions [1], [6] follow as special cases of LCP-A, when  $K$  is a power of two. The matrix  $\Theta$  in LCP-A can, in general, be written as a Vandermonde matrix

$$\Theta = \frac{1}{\beta} \begin{bmatrix} 1 & \alpha_1 & \cdots & \alpha_1^{K-1} \\ 1 & \alpha_2 & \cdots & \alpha_2^{K-1} \\ \vdots & \vdots & & \vdots \\ 1 & \alpha_K & \cdots & \alpha_K^{K-1} \end{bmatrix} \quad (26)$$

where  $\beta$  is a normalization factor chosen to impose the power constraint  $\text{tr}(\Theta\Theta^H) = K$ , and the selection of parameters  $\{\alpha_k\}_{k=1}^K$  depends on  $K$ , as follows.

R1) If  $K$  is an Euler number, i.e.,  $K \in \mathcal{K}_1 := \{\phi(P) : P \neq 0 \pmod{4}\}$  with  $\phi(P)$  denoting the number of positive integers that are less than  $P$  and relatively prime to  $P$ , then  $\{\alpha_k\}_{k=1}^K$  are roots of the equation  $\psi_P(x) = 0$ , where  $\psi_P(x)$  is defined as  $\psi_P(x) = \prod_{p \in \mathcal{P}} (x - e^{j2\pi p/P})$ , with  $\mathcal{P} := \{p : \text{gcd}(p, P) = 1 \text{ and } p \in [1, P)\}$ .

R2) If  $K$  is a power of two, i.e.,  $K \in \mathcal{K}_2 := \{2^p : p \in \mathbb{N}\}$  with  $\mathbb{N}$  denoting the set of positive integers,  $\{\alpha_k\}_{k=1}^K$  are chosen to be roots of  $x^K - \sqrt{-1} = 0$ . In this case,

$\Theta$  is a unitary matrix and can be compactly expressed as

$$\Theta = \mathbf{F}_K \text{diag}(1, \alpha_1, \dots, \alpha_1^{K-1}) \quad (27)$$

which turns out to coincide with those proposed in [1], [6], and [7].

R3) If  $K \notin \mathcal{K} := \mathcal{K}_1 \cup \mathcal{K}_2$ , then  $\{\alpha_k\}_{k=1}^K$  are chosen as roots of  $x^K - (1 + \sqrt{-1}) = 0$ .

For the reader's convenience, Table I lists the designs for  $K = 2, 3, \dots, 8$ . It is important to point out that the designed  $\Theta$  is not unitary when  $K$  is not a power of two, i.e., when  $K \notin \mathcal{K}_2$ . In general, the constellation precoding should not be interpreted as a constellation rotation.

The designed GLCP matrices  $\Theta$  in (26) satisfy C1) and C2). Regarding their performance, the following theorem is established [20].

*Theorem 1:* Consider a QAM (or PAM, or BPSK, or QPSK) constellation  $\mathcal{A}_s$  with minimum distance among signal points  $\Delta_{\min}$ . For the GLCP  $\Theta$  in (26), the achieved  $\xi_{\text{lcp}}$  is given by

$$\xi_{\text{lcp}} = \left[ \frac{\Delta_{\min}^2}{\beta^2} \right]^K$$

where

$$\beta^2 = \begin{cases} K, & \text{if } K \in \mathcal{K}_1 \cup \mathcal{K}_2 \\ \frac{1}{2^{K-1}}, & \text{otherwise.} \end{cases}$$

According to (25) and *Theorem 1*, we infer the following.

- 1) For  $K \in \mathcal{K}$ , GLCP-OFDM achieves maximum possible diversity and coding gains offered by LCP-OFDM.
- 2) For  $K \notin \mathcal{K}$ , GLCP-OFDM achieves maximum possible diversity gain but cannot achieve maximum possible coding gain. However, since  $(2^{1/K} - 1) \geq (\ln 2)/K$ , GLCP-OFDM can achieve at least 70% of the maximum possible coding gain  $G_{c, \max}$ . Whether there exists  $\Phi$  achieving  $G_{c, \max}$  for  $P = MK$  with  $K \notin \mathcal{K}$  is still an open question. Therefore, one should not conclude that subcarrier grouping induces a loss in the coding gain even when  $K \notin \mathcal{K}$ .

So far, we have discussed the construction of GLCP matrices  $\Theta$  that guarantees maximum possible diversity and coding gains when  $K = (L + 1) \in \mathcal{K}$ . In practice, however, the channel order  $L$  is a parameter determined by the underlying physical channel, and therefore,  $(L + 1) \in \mathcal{K}$  is not always satisfied. In other words, if one chooses  $K = L + 1$  for minimum decoding complexity, a maximum 30% loss in the coding gain is possible. Alternatively, one could choose the smallest  $K \notin \mathcal{K}$  such that

$K \geq L + 1$ , and then, construct our  $K \times K$  GLCP matrix  $\Theta$  according to (26). We have verified numerically that the so-chosen GLCP does achieve maximum coding gain, although we have not been able to provide a general proof that certainly constitutes an interesting future research topic. However, as implied by *Theorem 1*, the improvement is marginal (at most, 30% gain in the coding gain), and it is achieved at the expense of higher decoding complexity. In a nutshell, the choice of  $K$  depends on the tradeoff between performance and complexity.

### B. Symbol Detectability

Maximum diversity and coding gains are important when focusing on average performance of random fading channels. In practice, especially when fading channels do not change very rapidly, worst-case performance is of primary concern. In such cases, ensuring symbol detectability becomes extremely important. Symbol detectability means that information symbols can be detected correctly in the noise-free case, regardless of the underlying fading channel realization. We next discuss how our design is capable of ensuring that this property holds (see also [17]).

Due to subcarrier grouping, the equivalent channel vector  $\tilde{\mathbf{h}}_m := [H(p_{m,1}), \dots, H(p_{m,L+1})]^T$  is linked to  $\mathbf{h}$  via  $\tilde{\mathbf{h}}_m = \mathbf{U}_m \mathbf{h}$ . Because  $\mathbf{U}_m$  has full column rank under (24), it follows that  $\exists k' \in [1, K]$ , so that  $H(p_{m,k'}) \neq 0$  after excluding the trivial case  $\mathbf{h} \equiv \mathbf{0}$ . On the other hand, the design criterion C1 ensures that  $\forall s_m \neq s'_m$  it holds that  $\tilde{s}(nP + p_{m,k'}) \neq \tilde{s}'(nP + p_{m,k'})$ . Recalling (15), we then have  $y(nP + p_{m,k'}) \neq y'(nP + p_{m,k'})$  in the absence of noise, regardless of  $\mathbf{h}$ . This implies that we can always recover  $s_m$  from  $\mathbf{y}_m$ , uniquely. Regarding the relation between maximum diversity and symbol detectability, it is important to remark that maximum diversity implies symbol detectability, but the converse is not always true. Maximum diversity is an ensemble property pertaining to random fading channels, while symbol detectability is a deterministic property applicable to every channel realization.

## VI. COMPARISON WITH EXISTING ALTERNATIVES

LCP-OFDM has been designed to achieve maximum diversity and high coding gains with guaranteed symbol detectability, and relatively low decoding complexity. In this section, we further justify our design by comparing it with existing alternatives.

### A. Comparison With [16] and [17]

Linearly precoded OFDM (LP-OFDM) was originally proposed to maximize diversity gain and guarantee symbol detectability. Different from LCP-OFDM, symbol detectability in LP-OFDM does not depend on the underlying signal constellation, which may become useful when LP-OFDM is combined with channel coding. However, to ensure maximum diversity gain, LP-OFDM<sup>3</sup> sacrifices a bandwidth efficiency loss as compared to LCP-OFDM, and it relies on ML decoding whose complexity is exponential in the number of subcarriers

<sup>3</sup>This paper focuses on *multicarrier* transmissions, and our discussion here excludes the zero-padded (ZP) case in [17], which is basically a single-carrier transmission scheme. Low-complexity Viterbi decoding can be applied to ZP-only block transmissions to ensure maximum multipath diversity and coding gains [17], [18].

(or it is polynomial in the number of subcarriers if sphere decoding is applied). Because the number of subcarriers is larger than the channel order, LP-OFDM comes with high decoding complexity, unless one resorts to suboptimal linear [zero-forcing or minimum mean-square error (MMSE)] or nonlinear decision-feedback equalizers.

### B. Comparison With [7]

Targeting PAR reduction and performance enhancement, multidimensional signal sets were designed in [7] based on nonconvex optimization implemented by nonlinear search. In the framework of GLCP-OFDM, [7] corresponds to choosing  $K = 2^p$ ,  $p \in \mathbb{N}$ , and designing

$$\Theta = \mathbf{F}_K \text{diag}(e^{j\phi_1}, \dots, e^{j\phi_K}) \quad (28)$$

where the parameters  $\{\phi_k\}_{k=1}^K$  are obtained via computer search so that  $\xi_{\text{LCP}}$  is maximized. As expected, the optimum  $\Theta$  coincides with (26). As  $K = 2^p$  is only a subset of  $\mathcal{K}$ , GLCP-OFDM subsumes [7] as a special case. This also implies as a by-product that GLCP-OFDM also reduces PAR when  $K = 2^p$ . On the other hand, because [7] requires  $K = 2^p$ , a smaller  $K$  is possibly chosen by our design in certain cases. Hence, our design may yield lower decoding complexity than [7]. Moreover, our GLCP is constructed via closed-form algebraic methods, which are certainly simpler to design than the computer search, especially when a large signal constellation is used.

### C. Comparison With [12]

After optimal subcarrier grouping, our LCP-OFDM design amounts to designing  $\Theta$  for each GLCP-OFDM. At first glance, the GLCP-OFDM model (19) appears identical to [12, eq. (2)], where the diversity transform (DRT) matrix  $\mathbf{A}$  plays a role similar to  $\Theta$ . However,  $\mathbf{A}$  in [12, eq. (2)] is real and orthonormal, whereas our  $\Theta$  is, in general, complex and may be nonunitary.

But the distinction between our approach and [12] goes well beyond the complex versus real precoder used. In LCP-OFDM,  $\Theta$  is constructed to optimize diversity and coding gains, where the DRT matrix in [12] is constructed to maximize the channel cutoff rate. Different from PEP, the cutoff rate provides a lower bound on the Shannon channel capacity and also specifies an upper bound on the error probability of an optimal decoder at a fixed transmission rate [10, eq. (6)]. In addition to optimizing the DRT, [12] also considered a suboptimal linear diversity transform (LDRT) along with an MMSE detector having low complexity in the order of  $K^3$ . On the other hand, the expected complexity of sphere decoding that LCP-OFDM relies on is in the order of  $K^\alpha$ , where  $3 \leq \alpha \leq 4$  [8]. Therefore, for moderate values of  $K$ , the decoding complexity of GLCP-OFDM is comparable to LDRT. Targeting optimal performance, we will not optimize GLCP for linear detection. In our simulations, however, we will test how GLCP-OFDM performs when both optimal DRT and LDRT are used as GLCP.

## VII. DESIGN CONSIDERATIONS

So far, we have designed LCP-OFDM to enable maximum multipath diversity and coding gains with guaranteed symbol

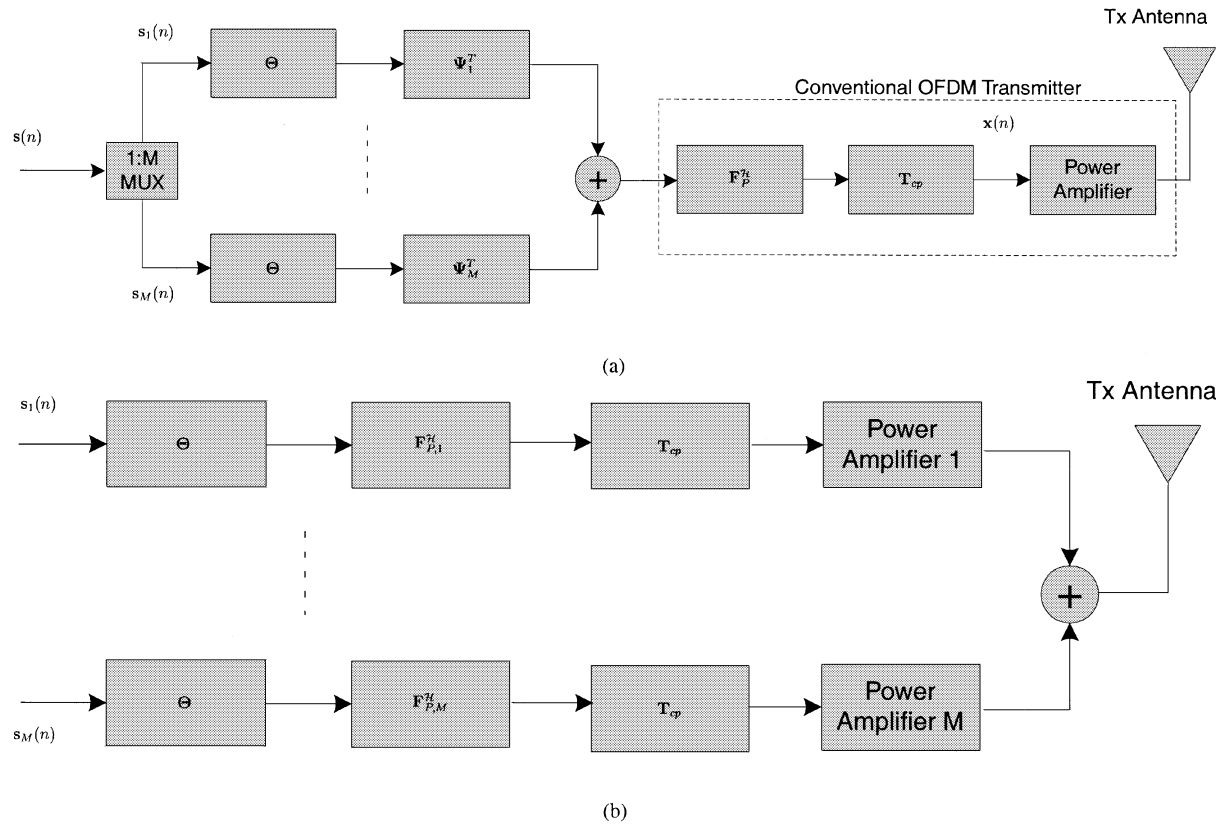


Fig. 3. (a) LCP-OFDM with uncoded OFDM. (b) LCP-OFDM for PAR reduction.

detectability and low decoding complexity. In this section, we consider several issues affecting the system performance and implementation of GLCP-OFDM.

#### A. Effects of Channel Overestimation

Our design of GLCP-OFDM is based on the assumption that the underlying channel  $\mathbf{h}$  is FIR of known fixed order  $L$ , which is rather idealistic for typical wireless applications. Without feedback from the receiver, the exact  $L$  is unknown at the transmitter. Moreover,  $L$  may change with time, depending on the location of the mobile communicators. The more realistic scenario is that one knows an upper bound  $\bar{L}$  and a lower bound  $\underline{L}$  of the channel order, i.e.,  $\underline{L} \leq L \leq \bar{L}$ . In order to achieve maximum diversity gain of order  $L + 1$ , it is clear from our discussion in Section IV that we should choose  $K$  for GLCP-OFDM based on  $\bar{L}$  instead of  $\underline{L}$ . Interestingly, our simulations will verify that this design (based on  $\bar{L}$ ) is still capable of achieving the coding gain in (14), which indicates that our LCP-OFDM in Sections IV and V is quite robust against channel overestimation. Note that the optimal subcarrier grouping is crucial to ensuring this robustness. Nevertheless, channel overestimation still induces higher decoding complexity than what is necessary.

#### B. Implementation Variants

In addition to low decoding complexity, the subcarrier grouping also brings flexibility into the system implementation, as we describe next.

Let  $\mathbf{T}_{cp} := [\mathbf{I}_{cp}^T \mathbf{I}_P^T]^T$  denote the operation of inserting the CP in OFDM, where  $\mathbf{I}_{cp}$  is formed by the last  $L_{cp}$  rows of the  $P \times P$  identity matrix  $\mathbf{I}_P$  [16]. In GLCP-OFDM, the transmitted baseband signal, denoted as  $\mathbf{x}(n)$ , is given by either

$$\mathbf{x}(n) = \mathbf{T}_{cp} \mathbf{F}_P^H \sum_{m=1}^M \Psi^T \Theta \Psi \mathbf{s}_m(n) \quad (29)$$

or

$$\mathbf{x}(n) = \sum_{m=1}^M \mathbf{T}_{cp} \mathbf{F}_{P,m}^H \Theta \mathbf{s}_m(n) \quad (30)$$

where  $\mathbf{F}_{P,m}^H := \mathbf{F}_P^H \Psi_m^T$  is a  $P \times (L+1)$  truncated IFFT matrix. Although (29) and (30) are mathematically equivalent, they lead to different implementations, as illustrated in Fig. 3(a) and (b).

The first implementation in Fig. 3(a) can be thought of as a direct enhancement to the conventional OFDM. Because the conventional OFDM transmitter is kept intact, this implementation requires little extra hardware investment. However, by keeping the conventional OFDM transmitter, the first implementation also inherits the drawbacks associated with conventional OFDM. One drawback is the large PAR associated with the linear combinations of  $P$  symbols at the IFFT output. In order to reduce PAR, one can choose  $K = 2^p$ ,  $p \in \mathbb{N}$ , and design  $\Theta$  according to (27), as suggested in [7].

The second implementation in Fig. 3(b) is in the spirit of the clustered OFDM system proposed in [3]. By checking the dimensionality of  $\mathbf{F}_{P,m}^H$ , the outputs of  $\mathbf{F}_{P,m}^H$  are linear combinations of only  $K$  symbols. Thus, the PAR is reduced considerably

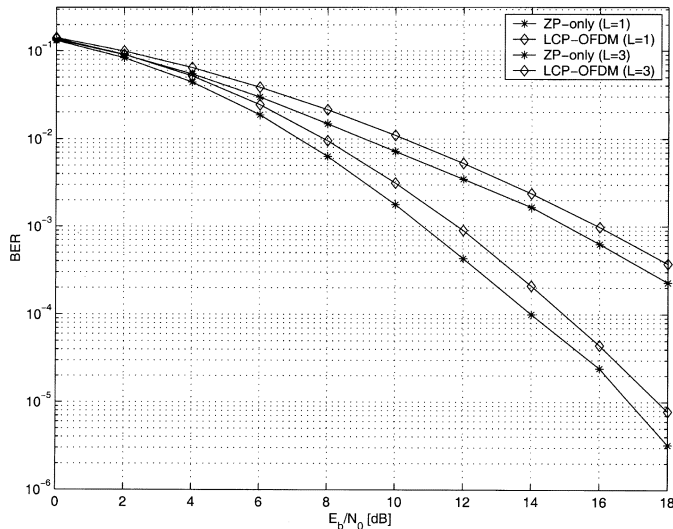


Fig. 4. LCP-OFDM versus ZP-only.

in the second implementation. This translates into cheap power amplifiers and performance improvement, as discussed in [3]. Furthermore, if we consider each branch in Fig. 3(b) as a user, the second implementation can be viewed as an LCP variant of the generalized multicarrier (GMC) code-division multiple-access (CDMA) scheme in [16] for multiuser systems, with the unique capability of supporting multiuser interference-resilient transmissions through frequency-selective (uplink or downlink) channels. In addition, by using different constellation sets for each of the  $M$  branches in Fig. 3(b), our second implementation supports multirate services. However, the second implementation may require additional signal isolators to isolate the collector terminal of power amplifiers from the summed signals. The cost of those signal isolators is an issue one should take into account in the second implementation.

### VIII. SIMULATIONS

In addition to theoretical analysis, we carry out simulations to investigate the performance of LCP-OFDM by choosing BER as our figure of merit. We employ QPSK modulation, and use the sphere decoding (SD) algorithm for near-ML decoding [15]. Unless specified otherwise, the fading channels are generated according to the assumption A2) with  $\mathbf{R}_h = (1/(L+1))\mathbf{I}_{L+1}$ , and they are assumed known to the receiver.

*Example 1 (Performance Comparison With LP-OFDM and ZP-only):* The pros and cons of C-OFDM versus LP-OFDM and ZP-only have been detailed in [17], where it is shown that at high code rates, both LP-OFDM and ZP-only have the potential to outperform C-OFDM in BER performance. Therefore, we only compare GLCP-OFDM with LP-OFDM and ZP-only. We choose  $P = 16$  and test two cases for  $L = 1$  and  $L = 3$ . The results in Fig. 4 show that ZP-only outperforms GLCP-OFDM marginally in both cases. It was proved in [18] that ZP-only achieves the same diversity and coding gains as LCP-OFDM. As mentioned before, the same amount of diversity and coding gains do not necessarily imply the same BER performance. The BER performance difference between ZP-only and LCP-OFDM is caused by other factors,

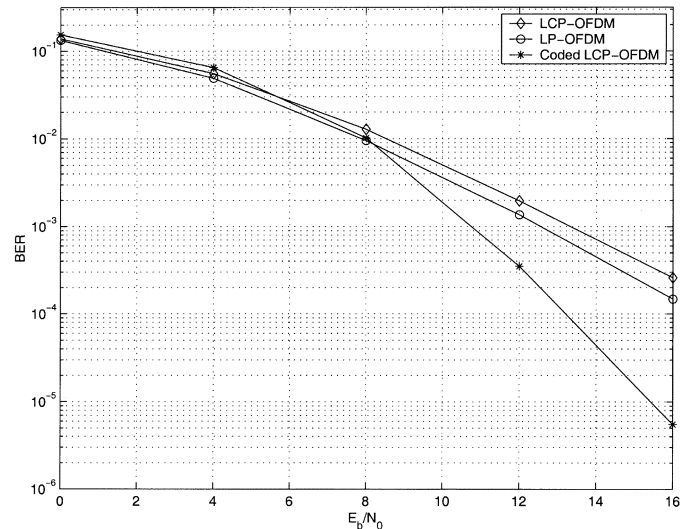


Fig. 5. LCP-OFDM versus LP-OFDM (cosine precoders).

such as the kissing number. Using parameters  $P = 15$  and  $L = 2$ , we further compare LCP-OFDM to LP-OFDM with the cosine precoders of [17] that result in a multicarrier scheme. As shown in Fig. 5, it is seen that LP-OFDM still outperforms LCP-OFDM slightly. However, in addition to higher decoding complexity, LP-OFDM has a lower transmission rate than LCP-OFDM. For fairness, we concatenate LCP-OFDM with a (15,13) Reed–Solomon coder (with block interleaving), so that both LCP-OFDM and LP-OFDM have the same transmission rate. Fig. 5 shows that coded LCP-OFDM outperforms uncoded LP-OFDM.

*Example 2 (Performance Comparison With [10]):* We replace GLCP in LCP-OFDM by either optimal DRT or LDRT. The resulting systems are termed as DRT-OFDM and LDRT-OFDM, respectively. The optimal DRT matrix  $\text{OP}_{2,4}$  in [12, Table I] is used in DRT-OFDM, while a normalized  $4 \times 4$  Hadamard matrix is used as LDRT. Two tests are carried out. The first test compares DRT-OFDM against LCP-OFDM, when both schemes use the SD algorithm. The second test compares LDRT-OFDM against LCP-OFDM, both with linear MMSE decoding. In all tests, we choose parameters  $P = 16$  and  $L = 3$ , and use BPSK modulation. The results in Fig. 6 illustrate that LCP-OFDM outperforms its DRT counterparts by more than 1 dB at  $\text{BER} = 10^{-3}$  in both tests.

*Example 3 (Improvements With Optimal Subcarrier Grouping):* To appreciate the importance of optimal subcarrier grouping, we choose parameters  $P = 64$  and  $L = 3$ , and compare the optimal subcarrier grouping with a suboptimal grouping specified by

$$\mathcal{I}_{m,\text{sub}} = \{(m-1)K+1, (m-1)K+2, \dots, mK\}.$$

It is observed in Fig. 7 that our optimal subcarrier grouping improves performance considerably. If we compute the coding gain under  $\mathcal{I}_{m,\text{sub}}$ , as compared to that under  $\mathcal{I}_{m,\text{opt}}$ , suboptimal subcarrier grouping will induce about 30-dB loss in the coding gain at high SNR.

*Example 4 (Effects of Channel Overestimation):* To investigate the robustness of LCP-OFDM against channel overesti-

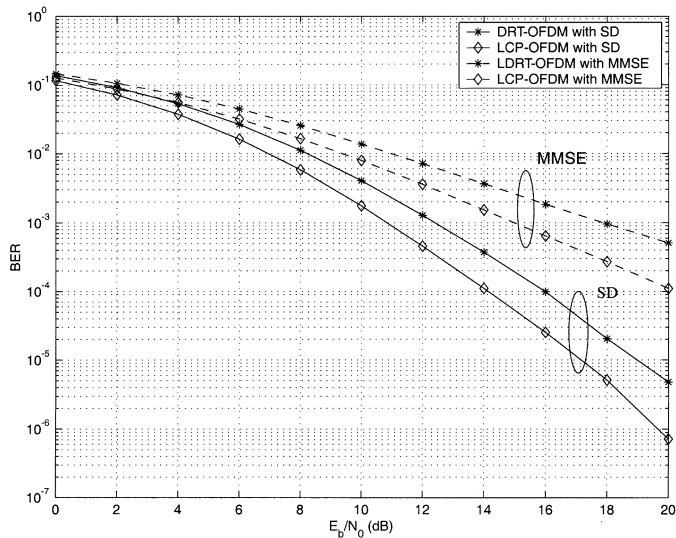


Fig. 6. LCP-OFDM versus (L)DRT-OFDM [10].

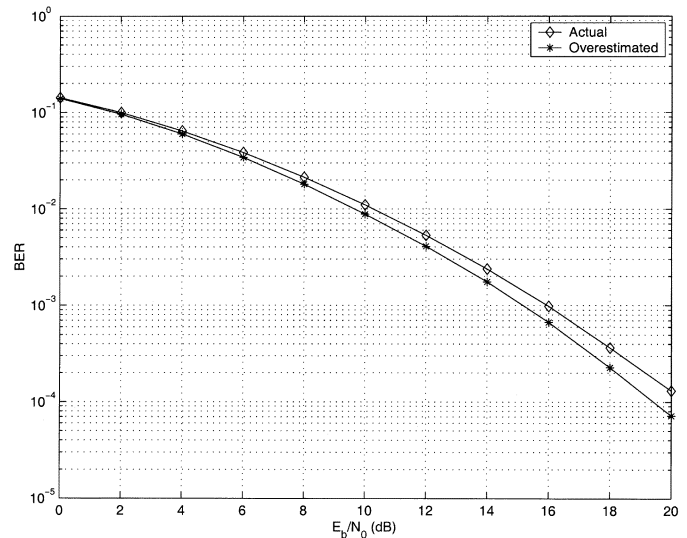


Fig. 8. Effects of channel overestimation.

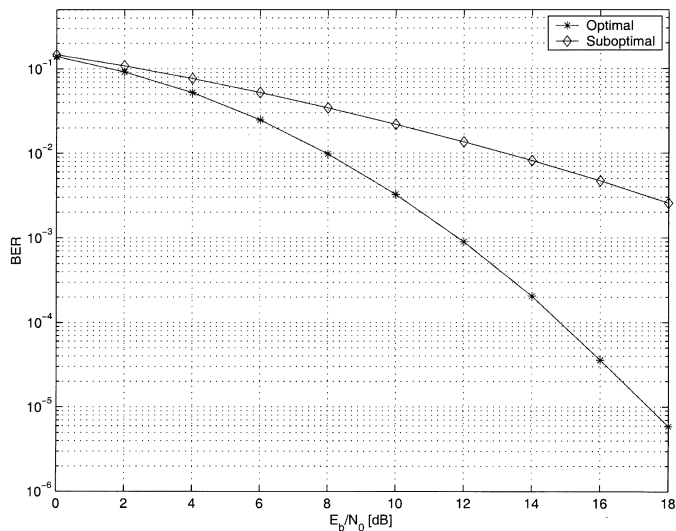


Fig. 7. Optimal versus suboptimal subcarrier grouping.

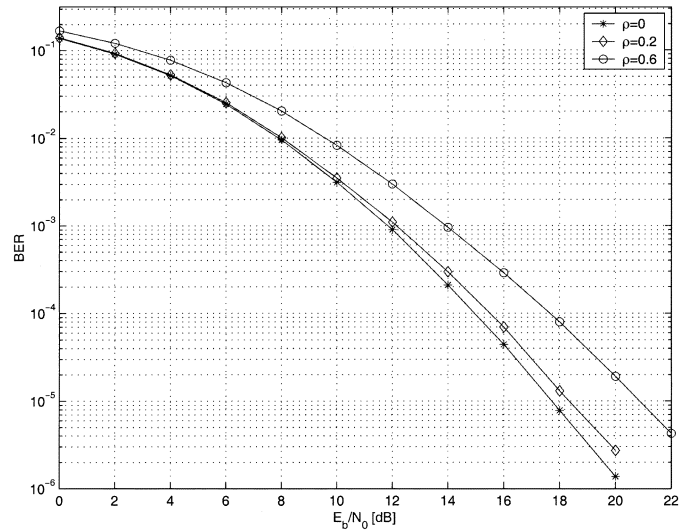


Fig. 9. Effects of channel correlation.

mation, we choose parameters  $\bar{L} = 3$ ,  $L = 1$ , and  $P = 12$ . We design two LCP-OFDM systems for both  $\bar{L}$  and  $L$ . Specifically, we choose  $K = 4$ ,  $\Theta_4$  for  $\bar{L}$ , while  $K = 2$  and  $\Theta_2$  are used for  $L$ . Interestingly, the comparison in Fig. 8 shows that the LCP-OFDM designed for  $\bar{L}$  outperforms that designed for  $L$ , although both systems have the same multipath diversity and coding gains. Again, we believe that the kissing number causes the difference.

*Example 5 (Effects of Channel Correlation):* We choose the following channel correlation matrix:

$$\mathbf{R}_h = \frac{1}{L+1} \begin{bmatrix} 1 & \rho & 0 & \cdots & 0 \\ \rho & 1 & \rho & \cdots & 0 \\ 0 & \rho & 1 & \cdots & 0 \\ \vdots & & & \ddots & \vdots \\ 0 & \cdots & \cdots & \rho & 1 \end{bmatrix}.$$

Selecting parameters  $P = 16$  and  $L = 3$ , we compare LCP-OFDM with i.i.d. channels (when  $\rho = 0$ ) to that with

correlated channels (when  $\rho = 0.2$  or  $\rho = 0.6$ ). It is seen from Fig. 9 that the channel correlation degrades BER performance noticeably. To improve performance with correlated channels, one could use a feedback channel to retrieve the information about channel correlation from the receiver, and adjust the precoder accordingly. Since channel correlations may change slowly, this information need not be updated frequently. Thus, not much loss in bandwidth efficiency will occur with feedback.

*Example 6 (Performance for HiperLan II Channels):* Selecting parameters  $P = 64$  and  $M = 8$ , we implement an LCP-OFDM for realistic channels ( $L = 7$ ) taken from the HiperLan II Channel Model A in [2]. The complexity of SD is polynomial in  $K = L + 1 = 8$ . In order to further reduce decoding complexity, we also implement another LCP-OFDM by splitting each group of  $K = 8$  subcarriers into two subgroups of four subcarriers, where a  $4 \times 4$  LCP is then designed. We compare these two implementations, and observe in Fig. 10 that the reduced complexity comes at the price of reduced but still acceptable performance. Our approach in this example provides

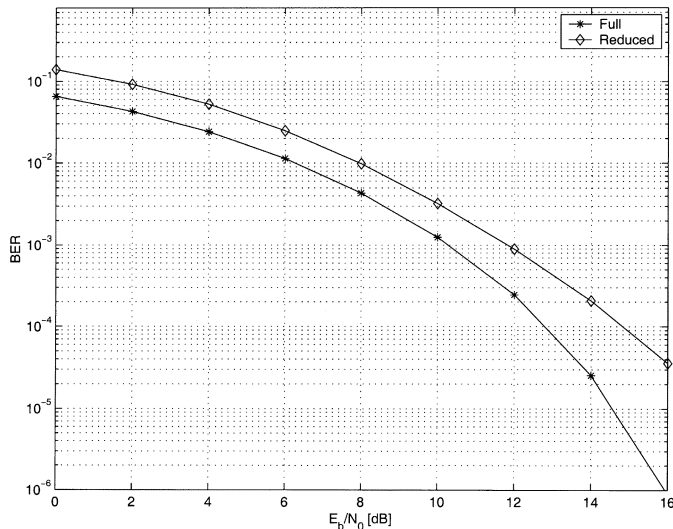


Fig. 10. Full- versus reduced-complexity LCP-OFDM.

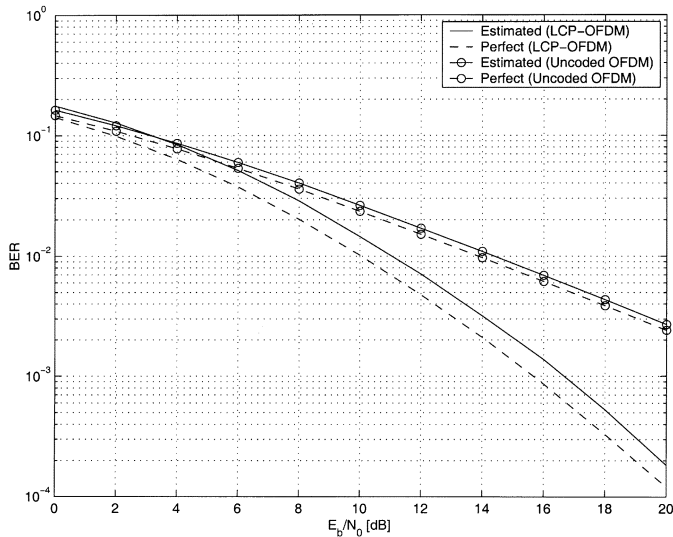


Fig. 11. Effects of imperfect channel estimates.

a way to trade off performance with complexity, which is useful in practice when long channels are encountered.

*Example 7 (Effects of Imperfect Channel Estimates):* Our previous simulations assume perfect CSI at the receiver. To investigate the effects of imperfect CSI, we simulate the BER of LCP-OFDM when channels are estimated using the standard least square channel estimator reported in [14]. We select parameters  $P = 16$  and  $L = 1$ . The BER of LCP-OFDM with estimated channels is shown against that with perfect CSI in Fig. 11, where we observe that imperfect channel estimates entail about 1-dB loss at  $\text{BER} = 10^{-3}$ . A similar result is also observed for uncoded OFDM in Fig. 11.

## IX. CONCLUSION

We proposed a novel OFDM scheme for multicarrier transmissions over frequency-selective channels using LCP. Relying on subcarrier grouping, we first converted the LCP-OFDM system into a set of GLCP-OFDM subsystems, and then

designed LCPs for each subsystem. While greatly reducing the system complexity, we proved that subcarrier grouping does not decrease the maximum possible diversity and coding gains. The proposed system was shown capable of achieving the maximum multipath diversity, large coding gains, and guaranteeing symbol detectability with low decoding complexity. In addition, the proposed system offers considerable flexibility as confirmed by simulations.

The proposed system works with a single transmit antenna. Extension to multiple transmit antennas equipped with space-time codes is currently under investigation.

## REFERENCES

- [1] J. Boutros and E. Viterbo, "Signal space diversity: a power- and bandwidth-efficient diversity technique for the Rayleigh fading channel," *IEEE Trans. Inform. Theory*, vol. 44, pp. 1453–1467, July 1998.
- [2] ETSI Normalization Committee, Channel models for HIPERLAN/2 in different indoor scenarios, Doc. 3ER1085B, Eur. Telecommun. Standards Inst., Sophia-Antipolis, France, 1998.
- [3] B. Daneshrad, L. J. Cimini, and M. Carloni, "Clustered OFDM transmitter implementation," in *Proc. IEEE Int. Symp. Personal, Indoor and Mobile Radio Communications*, vol. 3, Taipei, Taiwan, Oct. 15–18, 1996, pp. 1064–1068.
- [4] V. M. DaSilva and E. S. Sousa, "Fading-resistant modulation using several transmitter antennas," *IEEE Trans. Commun.*, vol. 45, pp. 1236–1244, Oct. 1997.
- [5] D. Divsalar and M. K. Simon, "The design of trellis-coded MPSK for fading channels: performance criteria," *IEEE Trans. Commun.*, vol. 36, pp. 1004–1021, Sept. 1988.
- [6] X. Giraud, E. Boutillon, and J. C. Belfiore, "Algebraic tools to build modulation schemes for fading channels," *IEEE Trans. Inform. Theory*, vol. 43, pp. 938–952, May 1997.
- [7] D. L. Göeckel and G. Ananthaswamy, "On the design of multidimensional signal sets for OFDM systems," *IEEE Trans. Commun.*, vol. 50, pp. 442–452, Mar. 2002.
- [8] B. Hassibi and H. Vikalo, "On the expected complexity of sphere decoding," in *Proc. 35th Asilomar Conf. Signals, Systems, and Computers*, Pacific Grove, CA, Oct. 29–Nov. 1, 2001.
- [9] J. F. Helard and B. Le Floch, "Trellis-coded orthogonal frequency-division multiplexing for digital video transmission," in *Proc. Global Telecommunications Conf.*, vol. 2, Phoenix, AZ, Dec. 2–5, 1991, pp. 785–791.
- [10] A. O. Hero and T. L. Marzetta, "Cutoff rate and signal design for the quasi-static Rayleigh fading space-time channel," *IEEE Trans. Inform. Theory*, vol. 47, pp. 2400–2416, Sept. 2001.
- [11] Y. H. Jeong, K. N. Oh, and J. H. Park, "Performance evaluation of trellis-coded OFDM for digital audio broadcasting," in *Proc. IEEE Region 10 Conf.*, Cheju Island, South Korea, Sept. 15–17, 1999, pp. 569–572.
- [12] D. Rainish, "Diversity transform for fading channels," *IEEE Trans. Commun.*, vol. 44, pp. 1653–1661, Dec. 1996.
- [13] V. Tarokh, N. Seshadri, and A. R. Calderbank, "Space-time codes for high data rate wireless communication: performance criterion and code construction," *IEEE Trans. Inform. Theory*, vol. 44, pp. 744–765, Mar. 1998.
- [14] J.-J. van de Beek, O. Edfors, M. Sandell, S. K. Wilson, and P. O. Björnsson, "On channel estimation in OFDM systems," in *Proc. Vehicular Technology Conf.*, Chicago, IL, July 25–28, 1995.
- [15] E. Viterbo and J. Boutros, "A universal lattice code decoder for fading channels," *IEEE Trans. Inform. Theory*, vol. 45, pp. 1639–1642, July 1999.
- [16] Z. Wang and G. B. Giannakis, "Wireless multicarrier communications: where Fourier meets Shannon," *IEEE Signal Processing Mag.*, vol. 17, pp. 29–48, May 2000.
- [17] —, "Complex-field coding for OFDM over fading wireless channels," *IEEE Trans. Inform. Theory*, vol. 49, pp. 707–720, Mar. 2003.
- [18] Z. Wang, X. Ma, and G. B. Giannakis, "OFDM or single-carrier zero-padded block transmissions," in *Proc. Wireless Communications and Networking Conf.*, vol. 2, Orlando, FL, Mar. 17–21, 2002, pp. 660–664.
- [19] Y. Xin, Z. Wang, and G. B. Giannakis, "Space-time constellation-rotating codes maximizing diversity and coding gains," in *Proc. Global Telecommunications Conf.*, San Antonio, TX, Nov. 25–29, 2001, pp. 455–459.

- [20] —, “Space–time diversity systems based on linear constellation precoding,” *IEEE Trans. Wireless Commun.*, vol. 2, pp. 294–309, Mar. 2003.
- [21] W. Zou and Y. Wu, “COFDM: an overview,” *IEEE Trans. Broadcast.*, vol. 41, pp. 1–8, Mar. 1995.



**Zhiqiang Liu** (M'02) received the B.S. degree from the Department of Radio and Electronics, Peking University, Beijing, China, in 1991, the M.E. degree from the Institute of Electronics, Chinese Academy of Science, Beijing, China, in 1994, and the Ph.D. degree from the Department of Electrical and Computer Engineering, University of Minnesota, Minneapolis, in 2001.

From 1995 to 1997, he worked as a research scholar at the Department of Electrical Engineering, National University of Singapore. From 1999 to

2001, he was a Research Assistant with the University of Minnesota, Minneapolis. He is now an Assistant Professor with the Department of Electrical and Computer Engineering, University of Iowa, Ames. His research interests lie in the areas of wireless communications and signal processing, including space–time coding, diversity techniques, wideband wireless communication systems, multiuser detection, multicarrier, and blind channel estimation algorithms.



**Yan Xin** (S'00) received the B.E. degree in electronics engineering from Beijing Polytechnic University, Beijing, China, in 1992, and the M.Sc. degrees in mathematics and electrical engineering from the University of Minnesota, Minneapolis, in 1998 and 2000, respectively. He is currently working toward the Ph.D. degree in the the Department of Electrical and Computer Engineering, University of Minnesota.

His research interests include space–time coding, diversity techniques, and multicarrier transmissions.



**Georgios B. Giannakis** (S'84–M'86–SM'91–F'97) received the Diploma in electrical engineering from the National Technical University of Athens, Greece, in 1981. He received the M.Sc. degree in electrical engineering in 1983, M.Sc. degree in mathematics in 1986, and the Ph.D. degree in electrical engineering in 1986, from the University of Southern California (USC), Los Angeles.

His general interests span the areas of communications and signal processing, estimation and detection theory, time-series analysis, and system identification, subjects on which he has published more than 150 journal papers, 300 conference papers, and two edited books. Current research focuses on transmitter and receiver diversity techniques for single- and multiuser fading communication channels, complex-field and space–time coding, multicarrier, ultra-wideband wireless communication systems, cross-layer designs, and distributed sensor networks.

Dr. Giannakis is the corecipient of four Best Paper Awards from the IEEE Signal Processing (SP) Society (1992, 1998, 2000, and 2001). He also received the Society's Technical Achievement Award in 2000. He co-organized three IEEE-SP Workshops, and guest co-edited four special issues. He has served as Editor in Chief for the IEEE SIGNAL PROCESSING LETTERS, as Associate Editor for the IEEE TRANSACTIONS ON SIGNAL PROCESSING and the IEEE SIGNAL PROCESSING LETTERS, as secretary of the SP Conference Board, as member of the SP Publications Board, as member and vice-chair of the Statistical Signal and Array Processing Technical Committee, and as chair of the SP for Communications Technical Committee. He is a member of the Editorial Board for the PROCEEDINGS OF THE IEEE, and the steering committee of the IEEE TRANSACTIONS ON WIRELESS COMMUNICATIONS. He is a member of the IEEE Fellows Election Committee, the IEEE-SP Society's Board of Governors, and is a frequent consultant for the telecommunications industry.